LLNL-JRNL-411549

A magnetized, spherical plasma expansion in an inhomogeneous plasma: The transition from super to sub-Alfvenic

S. H. Brecht, D. W. Hewett, D. J. Larson

March 25, 2009

Geophysical Research Letters

A magnetized, spherical plasma expansion in an inhomogeneous plasma: The transition from super to sub-Alfvénic.

Stephen H. Brecht[1], Dennis W. Hewett and David J. Larson
LLNL, Livermore CA

Abstract: In this letter the transition of a strong 3-D collisionless shock into sub-Alfvénic waves is examined numerically. The transition occurs because the Alfvén speed eventually exceeds the shock speed, not because the shock runs out of energy. At this velocity transition, the shock disassembles into two types of waves: the usual compressional Alfvén wave and a left-hand polarized electromagnetic shear Alfvén wave. This later wave shows remarkable 3-D coherence, and preliminary analysis suggests that it is coupled to the strong electromagnetic waves that exist within the collisionless shock.

Introduction:
The collisionless expansion of energetic plasma into a magnetized background plasma is a situation common to many areas of plasma research, e.g. supernova expansions, solar flares, and plasma blow-off in pulsed power experiments. These dynamic configurations are often categorized by the ratio of the expansion speed to the local Alfvén speed, the Alfvén Mach number. Over a period of many years the physics of such expansions has been studied experimentally [1]-[9], observationally, and now computationally. Transitions between the super- and sub-Alfvenic environments have not been previously examined in part due to the difficulty of observing the configuration experimentally and the multiple time scales involved in the necessary simulations. Yet, high energy releases in the ionosphere [1], in experiments [2], and in the natural world (i.e. solar flares and CME[24]) undergo such transitions.

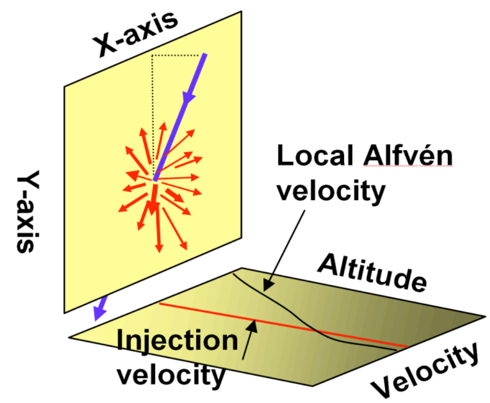

Figure 1. Schematic of the simulation geometry. The red arrows represent the spherically expanding driver plasma. The blue line is the ambient magnetic field line through the initiation point of the expansion.

Simulations of a collisionless shock, generated by a spherical, super-Alfvénic plasma injection into an inhomogeneous magnetized background plasma, gives rise to an unexpected rotational wave structure. This mode occurs when the shock enters a region in which the Alfvén velocity exceeds the shock speed. This constitutes the first numerical observation of this transition in a fully 3-D, inhomogeneous geometry.

A 3-D hybrid particle code is used to examine the transition of collisionless shocks to sub-Alfvénic waves. Using a simple super-Alfvénic, $v_{Shock} > v_A$, spherical expansion into an ionized, exponential-decreasing background, Fig. 1, one finds that a complex set of modes are generated in the sub-Alfvénic region. There is a portion of the shock front that transitions into a simple compressional Alfvén mode, perpendicular to the ambient magnetic field, and shear Alfvén waves directly along the ambient field line. The unexpected feature is that a portion of the shock front transitions into a left-hand polarized electromagnetic plasma mode. The mode is launched at

[1] Bay Area Research Corp

This work performed for the Defense Threat Reduction Agency contract DTRA IACRO 07-42261 and under the auspices of the U.S. Department of Energy by Lawrence Livermore National Laboratory in part under Contract No. W-7405-Eng-48 and in part under Contract DE-AC52-07NA27344.

an angle between the density gradient and the ambient magnetic field with a tendency to become field aligned. This letter briefly describes the simulation model and some of the characteristics of this new mode.

Discussion

The simulation model is a 3-D hybrid, Particle-In-Cell (PIC) code that assumes charge neutrality and models the electrons as an inertialess fluid. The ions are treated as kinetic macro-particles and advanced according to the Lorentz force law, thus including finite-gyro-radius effects. The fields are solved self-consistently on a spatial grid. The electric fields, **E,** are determined from the electron momentum equation in the inertia-less, quasi-neutral limit, $\overline{E} = \nabla p / en + \overline{u}_e x \overline{B} / c$. Faraday's law is used to advance the magnetic field, **B**. Light waves have been removed from the simulation by setting the displacement current to zero, cf: [10-12]. Details of this model and its numerical implementation are available in references [10,13].

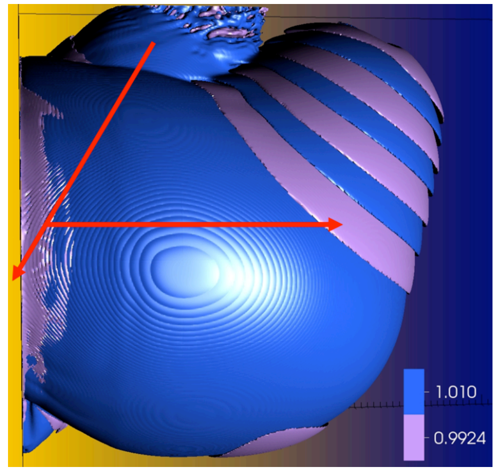

Figure 2. Surface plots of $\delta B / |B_0|$ reveal a helical mode emerging from a magnetic bubble. The first arrow is in the direction of the ambient B field and the horizontal arrow is in the opposite direction to the background plasma density gradient.

The energetic particles are injected spherically at v_{Shock}, and the Alfvén Mach number is 8. The background plasma has an exponential density gradient, such that the Alfvén speed exceeds the initial expansion speed roughly 120 cells above the initiation point. The background magnetic field is a constant at t = 0 and is tipped 30 degrees. The cell size is roughly 4 c/ω_{pi} at the initiation point and less than c/ω_{pi} at the altitude of shock transition. The simulations used roughly 300 million particles and over 50 million zones with outflow boundary conditions on all grid boundaries.

Results

The time evolution of the simulation reveals the unexpected development of a large coherent helical wave that grows from the expanding magnetic "bubble", Fig. 2. The helical mode is initially launched in a direction between the background density gradient and the direction of the ambient magnetic field (the two red lines in Fig. 2). The mode is left-hand polarized and the magnitude of the perturbed B is roughly one tenth of the ambient **B**. Fig. 2 shows contours slightly above and below the normalized ambient field strength. The mode is observed for a wide variety of injected plasma conditions (variations in charge state, various mixes of driver species, ion gyro-radii, etc). Numerical tests clearly show that the mode is not sensitive to the electron pressure term or to electron temperature gradients. Changing the scale height of the atmosphere does not affect the generation of this wave, nor does the charge state of the expanding plasma or even the number of ion species in the expanding plasma.

The development of this feature seems to be tied to the super-Alfvénic shock created in the background plasma by the injected plasma: sub-Alfvénic initial conditions do not produce this mode. The helical mode emerges as the collisionless shock encounters the region where the local Alfvén velocity becomes greater than v_{Shock}.

Collecting information at several spatial regions permits preliminary analysis of the modes, Fig._3. **A** is located in the helical mode region; **B** is located deeper in the interior along the path of the helical mode; **C** is in a region of nonlinear perpendicular propagating modes, see Table 1. For each region, time-dependent data was collected and analyzed using a power-spectral-density analysis.

Table 1

Parameters	ω/ω_{ci}	$ck_{\parallel}/\omega_{pi}$	V_{phase}/V_A	$\delta B_N / \lvert B_0\rvert$	$\delta B_{\parallel} / \lvert B_0\rvert$	$\delta B / \lvert B_0\rvert$
Region **A**	~2.4	~1.4	~1.45	~0.3	~0.33	~0.1
Region **B**	~1.06	~2.4	~0.96	~0.66	~2	~2
Region **C**	~1.94	~0	~1.22	~0.0	~2	~2

The normalization parameters used are the ones local to each individual collection region. The magnetic field was initialized with a constant value, $\mathbf{B_0}$, in all regions. All other parameters do change because the background density is decreasing with altitude, Fig 1. It should be noted that if the c/ω_{pi} at **B** is used to normalize the parallel wave number at **A**, then $ck_{\parallel}/\omega_{pi} \sim 2.6$ at **A**, which means the actual wave number is essentially the same in both regions.

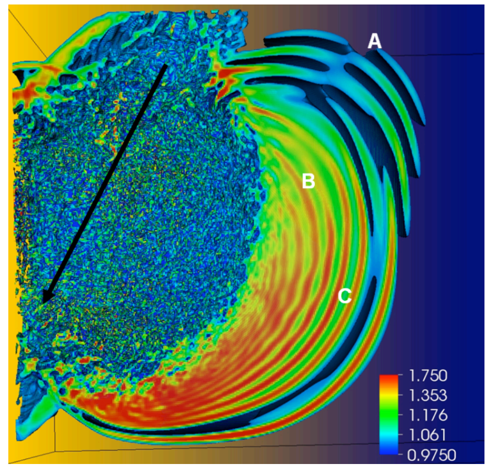

Figure 3. A cross-section of Fig. 2 showing the data collection points to be discussed. The legend is $\delta B / \lvert B_0 \rvert$.

Theoretical Considerations:

Collisionless shocks have been studied in nature (planetary bow shocks, interplanetary shocks cf. [14]) and via simulation (cf. [15], and references therein). These shocks are very turbulent and are created by reflecting ions which create an anisotropic pressure tensor ($P_{\perp}>P_{\parallel}$). Subsequently, electromagnetic instabilities anisotropize the ion pressure, consistent with both simulations [15] and theory [16]. The non-linear evolution of this ion pressure or temperature anisotropy driven mode, the Alfvén Ion Cyclotron or ion whistler mode, has also been studied [17]. This mode is a left-hand-polarized electromagnetic mode that propagates parallel to magnetic field lines.

As the shock and bubble expand outward, the Alfvén speed begins to increase to the right, Fig. 2, and this portion of the shock begins to disassemble when it exceeds the local Alfvén speed. Examination of Figs. 2 and 3 clearly show asymmetry in the modes propagating away from the shock region. The mode propagating through region **C**, Fig. 3, is a purely compressional mode with no change in the field component normal to the ambient field ($\delta B_N / \lvert B_0\rvert \sim 0$), Table 1. In the case of the new wave, region **A**, the mode displays ($\delta B_N / \lvert B_0\rvert \sim \delta B_{\parallel} / \lvert B_0\rvert$). In region **A,** the electric field and δB form a set of perpendicular rotating vectors.

Linear theory offers insight into the simulation results. From [16] one notes that $\omega_0 \sim \omega_{ci}\,(1 - T_{i\parallel}/T_{i\perp})^2$ and $k_0^2 \sim (\omega_{pi}^2 / c^2)((T_{i\perp} - T_{i\parallel})^2/(T_{i\parallel}\, T_{i\perp})$. Examining Fig. 3 of [16], reveals that $ck_{\parallel}/\omega_{pi} \sim 2.4$ corresponds to $\lvert\omega\rvert / \omega_{ci} \sim 1$. This is consistent with the results at **B**, where $\lvert\omega\rvert / \omega_{ci} \sim 1.06$. The results at **A** are not represented by the dispersion relation in [16]. The phase speed at **A** is substantially higher than the local Alfvén speed. In a monograph on Alfvén waves, [18 p. 47], it is noted that an Alfvén surface wave in a non-uniform plasma changes its dispersion relation from $\omega = k_{\parallel} v_A$ to $\omega = (2)^{1/2} k_{\parallel} v_A$. At **A** one finds that the measured phase speed of the waves is 1.45 times the local ambient Alfvén speed. Hasagawa[18] also notes this mode will be damped at high beta.

Examining Fig. 4 one sees that the field lines within the shocked region are connected to those in the direction of the wave propagation. This suggests the possibility of mode conversion between the parallel propagating AIC modes and the parallel propagating shear Alfvén modes especially since the dimensionless wavelengths seen at **A** and **B** are very similar, when normalized by the same c/ω_{pi}. Indeed [18] shows that the Alfvén mode does couple to the firehose instability which is the fluid version of the AIC/EMIC mode [16].

However, direct mode conversion is not the only possible source of this wave. Kinetic Alfvén waves can be generated in an inhomogeneous plasma with conditions that exist in the shock transition region, Lysak [23]. Although the frequency seen in the simulations is higher than in Lysak's analysis, the simulations may be showing the full 3-D structure of the kinetic Alfvén wave.

It should be noted that the ion gyroradius within the helical mode is much smaller than the size of the features. Further, in the region where the helical mode exists, there are no ions from the driver, nor are there any indications of beaming in the ion distribution functions.

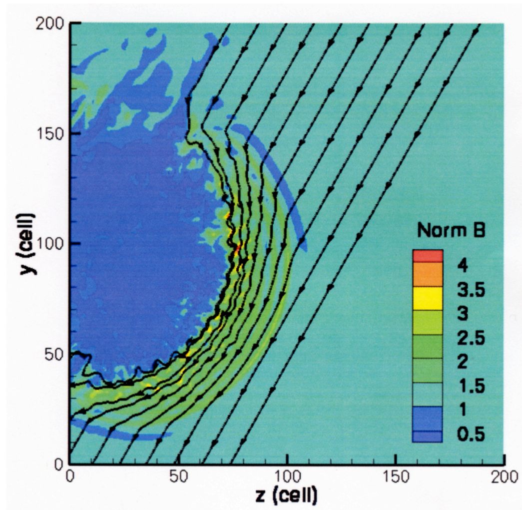

Figure 4. Magnetic field lines connect the internal region where the AIC mode is active to the external region where the helical mode will propagate. The legend is $|B|/|B_0|$.

SUMMARY:
The three dimensional simulation of a spherical super-Alfvénic expansion transitioning into a sub-Alfvénic flow has produced a surprising result. The most remarkable aspect of these results is that the mode created is very large scale and is extremely coherent. This effect appears to be purely a three dimensional result generated in spherical-like geometries; it is not seen in 2-D.

The highly coherent helical mode could be further investigated experimentally. Empirical evidence for this mode may have already been seen in rotational discontinuities in the solar wind, [19]. It is also likely that such behavior could be detected in laser target experiments [2, 20-22]. What is clear is that some mechanism is radiating energy from the short wave turbulent region to the large scale helical structure outside of the magnetic bubble, much like an antenna radiating a coherent wave.

Acknowledgements: The authors would like to acknowledge the assistance of Dr. Chester Eng and that of Ms. Ellen Tarwater.

This work was sponsored by the Defense Threat Reduction Agency under DTRA IACRO 07-42261 and under the auspices of the U.S. DOE by Lawrence Livermore National Laboartory under Contract No. DE-AC52-07NA27344

References:
[1] Dyal, P., *J. Geophys. Res.,* **111**, A12211, doi:10.1029/2006JA011827, 2006.
[2] Zakharov, Yu.P., *IEEE Transactions on Plasma Science,* **31**, 1243, 2003.
[3] Bostic, W.A., *Phys. Rev.,* **104**, 292, 1956.
[4] Bostic, W.A., *Phys .Rev.,* **106**, 104, 1957.

[5] Jellison, G. and C.R. Parsons, *Phys. Fluids,* **26**, 1171, 1983.
[6] Zakharov, Yu. P., A.M. Orishich, A.g. Ponomarenko, and V.G. Posukh, *Sov.J. Plasma Phys.*, **12**, 674, 1986.
[7] Ripin, B.H.E. *et al., Phys. Rev. Lett.*, **59**, 2299, 1987.
[8] Dimonte, G. and L.G. Wiley, *Phys. Rev. Lett.*, **67,** 1755.1991.
[9] Zakharov, Yu.P., *Plasma Phys. Reports,* **32,** 183, 2006.
[10] Harned, D.S., *J. Comp. Phys.*, **47**, 452 (1982).
[11] Hewett, D.W., *Computer Physics Communications,* **84**, 243, (1994).
[12] Brecht, S.H. and S.A. Ledvina, *Space Sci. Reviews*, **126**, doi:10.1007/s11214-006-9084-z, 15, (2006).
[13] Brecht, S.H., and V.A., Thomas, *Comp. Phys. Comm.*, **48,** 135, (1988).
[14] Bale, S.D, F.S. Mozer, and T.S. Horbury, *Phys. Rev. Lett.*, **91**, 265004-1, (2003).
[15] Thomas, V.A. and S.H. Brecht, *J. Geophys. Res.,* **92**, 3175, (1987).
[16] Davidson, R.C. and J.M. Ogden, *Phys. Fluids,* **18**, 1045, (1975).
[17] Ambrosiano and S.H. Brecht, *Phys. Fluids*, **30**, 108, (1987).
[18] Hasagawa, A., and C. Uberoi, The Alfvén Wave, Technical Information Center, U.S. Department of Energy, DOE/TIC-11197, (1982)
[19] Neugebauer, M. *J. Geophys. Res.,* **111**, A04103, doi:10.1029/2005JA011497, (2006).
[20] Gekelman, W., M. Van Zeeland, S. Vincena, and P. Pribyl, *J. Geophys. Res.,* **108**, doi:10.1029/2002JA009741, (2003).
[21] Vincena, S., W. Gekelman, and J. Maggs, *Phys. Rev. Lett.*, **93**, 0031-9007/04/93(10)/105003(4), (2004).
[22] Vincena, S., and W. Gekelman, *Phys. of Plasmas,* **13**, 1070-664X/13(6), 064503/4, (2006).
[23] Lysak, R. L., *Phys. Plasmas* **15** 062901 (2008).
[24] Mann, G., A.Klassen, H. Aurass, and H.T. Classen, “Development of Shock Waves in the Solar Corona and the Interplanetary Space,” *Solar Wind Ten: Proceedings of the Tenth International Solar Wind Conference,* Ed. M. Velli, R. Bruno, and F. Malara, AIP, 612, 2003.